Materials Chemistry and Physics 134 (2012) 789–796

Contents lists available at SciVerse ScienceDirect

Materials Chemistry and Physics

journal homepage: www.elsevier.com/locate/matchemphys

Effect of thermal aging on the optical, dynamic mechanical, and morphological properties of phenylmethylsiloxane-modified epoxy for use as an LED encapsulant

Chia-Wen Hsu [a,b], Chen-Chi M. Ma [a,*], Chung-Sung Tan [a], Hsun-Tien Li [b], Shu-Chen Huang [b], Tzong-Ming Lee [b], Hsin Tai [a]

[a] *Department of Chemical Engineering, National Tsing Hua University, Hsinchu 300, Taiwan, ROC*
[b] *Material and Chemical Research Laboratories, Industrial Technology Research Institute, Hsinchu, Taiwan, ROC*

ARTICLE INFO

Article history:
Received 2 September 2011
Received in revised form
8 February 2012
Accepted 13 March 2012

Keywords:
Optical materials
Aging
Mechanical properties
Electron microscopy

ABSTRACT

We investigated the thermal stability of the diglycidyl ether of bisphenol A (DGEBA)–methylhexahydrophtalic anhydride (MHHPA) modified with phenylmethylsiloxane-modified epoxy (PMSE) and the effects of this hybrid on the performance of light emitting diodes (LEDs). The optical and dynamic mechanical properties of the materials, and the effects of these properties on the light output from the encapsulated LEDs, were studied following long-term thermal aging at 150 °C. The DGEBA–PMSE hybrids were highly transparent and its optical stability was shown in the stable light output of the LED, which was 19% higher than that of LEDs encapsulated by DGEBA–MHHPA after 30 days. Molecular rearrangement occurred in the nanoscale domain of the hybrids after thermal aging, which caused the dynamic mechanical effect on the LED performance, as demonstrated by TEM. We observed the hybrid modified using 0.2 equivalents of PMSE possessed both optical and dynamic mechanical stability, and resulted in the most stable LED performance.

1. Introduction

Both epoxy and polysiloxane (silicone) are used commonly as encapsulants in light emitting diodes (LEDs). LEDs are used for a variety of lighting applications, including display backlighting, automotive lighting, large display panels, indoor and outdoor lighting. The properties of the high performance encapsulants that are used in LED devices are in need of improvement for advanced applications, such as LEDs of higher power. The encapsulants must be sufficiently robust to withstand the higher working temperatures found at p–n junctions and the accumulating heat within LEDs.

Encapsulants should be homogenous, optically transparent, and stable at high temperatures and under UV light [1]. In general, the optical properties of epoxies such as the diglycidyl ether of bisphenol A (DGEBA) allow these materials to be used as LED encapsulants, but unfortunately they undergo rapid degradation when exposed to high temperatures or UV light. The degradation in light output from an LED that is caused by yellowing of the epoxy depends on the high working temperature within LEDs, the amount of short-wavelength radiation to which the LED is exposed, and so forth [2].

The blend of polysiloxane to epoxy is one of the most common methods used to enhance the thermal stability and mechanical properties of epoxy [3–7]. However, most of polysiloxanes are immiscible with epoxy, and they are also difficult to form homogenous compounds between them due to the intrinsic solubility difference of these two kinds of polymer [8–11]. Therefore, the selection of polydimethylsiloxane (PDMS)-modified epoxy which possesses good compatibility with epoxy is an essential prerequisite for developing transparent LED encapsulant.

Previous investigation of the thermal aging effect on the decay of LED light output focus on the optical degradation of the encapsulant, and have scarcely touched on their mechanical properties. Some researchers have revealed the optical changes that occur in the encapsulant after storage at high temperatures for a long time [12–15]. Furthermore, it is clearly important to understand the correlation between the changes in the optical properties of the material and the changes in the light output of an LED device [16,17].

In this study, we used PDMS-modified epoxy such as phenylmethylsiloxane-modified epoxy (PMSE) which is compatible with DGEBA, and it was used to produce DGEBA–PMSE hybrids. We studied the optical and dynamic mechanical properties of this

---

* Corresponding author.
E-mail address: ccma@che.nthu.edu.tw (C.-C.M. Ma).

0254-0584/$ – see front matter © 2012 Elsevier B.V. All rights reserved.
doi:10.1016/j.matchemphys.2012.03.070

material and correlated them with the light output of an LED that had been subjected to long-term thermal aging at high temperatures. We also investigated the changes in the nanoscale morphology of DGEBA–PMSE hybrids that occurred during thermal aging. With the decay in the luminous flux of the LED, there was not only a decay in transmittance of the material, the dynamic mechanical properties of the material also changed due to the rearrangement of the DGEBA–PMSE molecules.

2. Experimental

2.1. Materials

The diglycidyl ether of bisphenol A (DGEBA) with an epoxide equivalent weight of 190 g/eq. was purchased from Eclat Applied Technology Co. Ltd, Taoyang County, R.O.C. (Phenylmethylsiloxane-co-dimethylsiloxane)-glycidyl ether terminated copolymer (phenylmethylsiloxane-modified epoxy, PMSE) with an epoxide equivalent weight of 680 g/eq. was purchased from Grand Tek Advance Material Science Co. Ltd., Taipei, R.O.C., and its structure is shown in Scheme 1. Methylhexahydrophthalic anhydride (MHHPA) was purchased from Eclat Applied Technology Co. Ltd, Taoyang County, R.O.C.. Quaternary phosphonium bromide (U-cat 5003) was purchased from San-Apro Ltd., Tokyo, Japan, and used as an accelerator of curing for the epoxy and anhydride. Activated carbon was purchased from Showa Co., Tokyo, Japan, and was used to purify the PMSE.

2.2. Purification of the PMSE

The PMSE was light yellow, and had an initial yellowness index of 10.91, as measured by spectrophotometer (SA2000, Nippon Denshoku, Industries Co., Ltd.). The PMSE was placed in a round-bottomed flask, and 3 g of activated carbon were added per 100 g of PMSE. After stirring for 24 h, the PMSE was filtered using a 0.2-μm polytetrafluoroethylene (PTFE) membrane was purchased from Whatman Inc., New Jersey, U.S.A.. Each batch of PMSE was purified three times. The purified PMSE was then placed in a vacuum oven at 80–100 °C under a reduced pressure to remove the water. The final yellowness index of the purified PMSE was 1.24.

2.3. Preparation of plate samples

Three different compositions of materials were used in our experiments. DGEBA–PMSE-0.2 was formed using the ratio DGEBA:PMSE:MHHPA = 0.8:0.2:1 by equivalent weight. DGEBA–PMSE-0.4 was formed using the ratio DGEBA:PMSE:MHHPA = 0.6:0.4:1 by equivalent weight. For comparison, DGEBA–MHHPA was formed using a ratio of 1:1 by equivalent weight. In all cases, the catalyst (U-cat 5003) was used 5% by weight of the total solution and dissolved in MHHPA at 50 °C for 60 min in a beaker. The DGEBA and PMSE were then added to the beaker and the mixture was stirred at room temperature until a homogeneous solution was formed. The bubbles were removed from the solution using a vacuum pump, and the solution was then cast in a mold made from two pieces of glass that were separated and sealed with a piece of silicone rubber that was 3 mm thick. After curing, the two pieces of glass were removed to give transparent plate samples of each material of dimensions 40 × 40 × 3 mm.

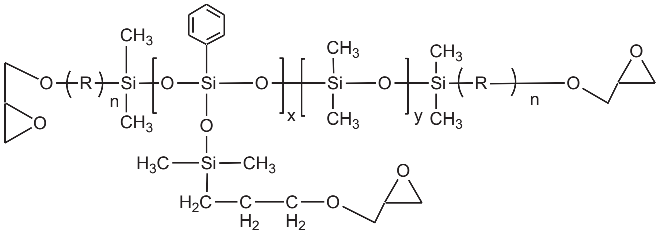

Scheme 1. (Phenylmethylsiloxane-co-dimethylsiloxane)-glycidyl ether terminated copolymer (PMSE).

2.4. Preparation of encapsulated LEDs

Lamp-type LED lead frames, each consisting of 20 wire-bonded blue LED chips (20 mA, emitting wavelength 460 nm), were purchased from Sander Electronics Co. Ltd., Taipei, R.O.C. The solutions described above were poured into the mold and the LED lead frame was then inserted into the mold. After curing, the lead frame was removed from the mold, which resulted in a total of 20 encapsulated LEDs for each material.

2.5. Analysis of long-term thermal aging

Both the plate samples and the encapsulated LEDs were placed in an oven at 150 °C and their properties were measured after 0, 10, 20, and 30 days of thermal aging.

2.6. Curing reaction behavior

The cured structures of the DGEBA–PMSE hybrids were analyzed using Fourier transform infrared spectroscope with the attenuated total reflectance sample accessory (FTIR-ATR; Spectrum One, PerkinElmer, Inc.). The scanning range was 650–4000 cm^{-1}. The absorption peaks were measured for different postcure conditions following precuring at 120 °C for 2 h, to determine the most suitable curing condition for each material.

The behavior and kinetics of the materials during the curing reaction were studied using differential scanning calorimetry (DSC; Q-10, TA Instruments, Inc.) under nitrogen gas. The solutions were measured by DSC at four different rates of heating, i.e., 10 °C, 12 °C, 15 °C and 17 °C min^{-1}. The exothermic peak of each reaction, and the activation energy of each curing reaction were analyzed using the Kissinger method [18].

2.7. Long-term thermal aging behavior

The optical properties of each material were measured using a spectrophotometer. Given that the wavelength of the LED device was approximately 460 ± 20 nm, we analyzed the stability of the transmittance of the plate samples at 450 nm during thermal aging.

The dynamic mechanical properties of the samples were measured using dynamic mechanical analysis (DMA; Q800, TA Instruments, Inc.) from −100 °C to 280 °C at a heating rate of 5 °C min^{-1} using a fixed frequency of 1 Hz.

The morphologies of the DGEBA–PMSE hybrids were examined using a transmission electron microscope (TEM; JEM-2100F, JEOL) operating at 200 kV. The samples were trimmed and stained with ruthenium tetroxide solution to enhance the contrast between the regions with and without aromatic rings.

The light output (luminous flux, lm) of the LEDs was measured using an integrating sphere (ISP 250, Instrument Systems). For each material, 20 encapsulated LEDs were tested.

3. Results and discussion

3.1. Curing behavior

The behavior of the materials during curing was measured using DSC. The DSC exothermic curves were plotted as a function of temperature, and the results are shown in Fig. 1. The exothermic curves first showed an increase around 100–120 °C, reached a maximum at around 163–165 °C and reduced to zero at around 200–220 °C. The peaks were broader when the epoxy was replaced partially by PMSE, and the heat flow decreased with the addition of increasing quantities of PMSE. The heat flows were 330, 300, and 230 W/g for DGEBA–MHHPA, DGEBA–PMSE-0.2, and DGEBA–PMSE-0.4, respectively. A precuring condition of 120 °C for 2h was chosen, and the optimal postcure condition was identified using FTIR-ATR.

3.2. Postcuring conditions

Fig. 2 shows the adsorption curves of each of the uncured solutions and each of the cured materials following different postcuring processes. The curing mechanism for epoxy and anhydride entails some changes in the absorptions of the functional groups [19]. The absorptions at 1860 and 1785 cm^{-1} corresponded to the C=O of anhydride, and disappeared in favor of an absorption at 1731 cm^{-1}, which corresponded to the C=O of an ester. For the uncured solution, the absorptions at 944 and 901 cm^{-1} corresponded to the phthalic anhydride C–O, and the absorption at 913 cm^{-1} corresponded to the epoxide stretching of C–O–C. In the cured materials, the absorptions at 944 cm^{-1}, 901 cm^{-1}, and 913 cm^{-1} were absent. The postcure condition of each material was assumed when the intensities of the absorption peaks did not change any further.

As seen in Fig. 2(a) and (b), the absorption curves of both DGEBA–MHHPA and DGEBA–PMSE-0.2 were stable with postcuring conditions of 150 °C for 3h. From Fig. 2(c), it may be seen that, for DGEBA–PMSE-0.4, the absorption at 913 cm^{-1} remained even with postcuring of 150 °C for 5h. However, the absorption at 913 cm^{-1} disappeared completely when a higher temperature of 160 °C for 3h was used for the postcuring. This result shows that hybrids that have higher PMSE contents require a higher temperature for postcuring. The PMSE reduces the reactivity of the hybrid during curing, as determined using Kissinger method.

3.3. Curing kinetics

The curing kinetics of DGEBA–MHHPA, DGEBA–PMES-0.2, and DGEBA–PMES-0.4 were studied at various heating rates using the Kissinger method, wherein the activation energy of the curing

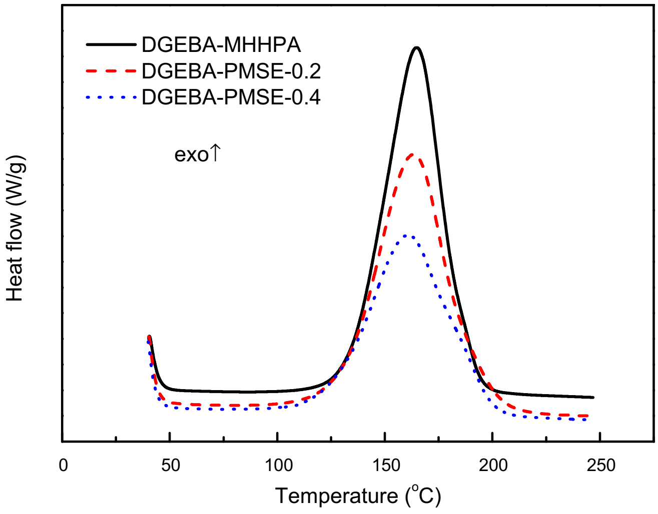

Fig. 1. The DSC exothermic curves of the three materials.

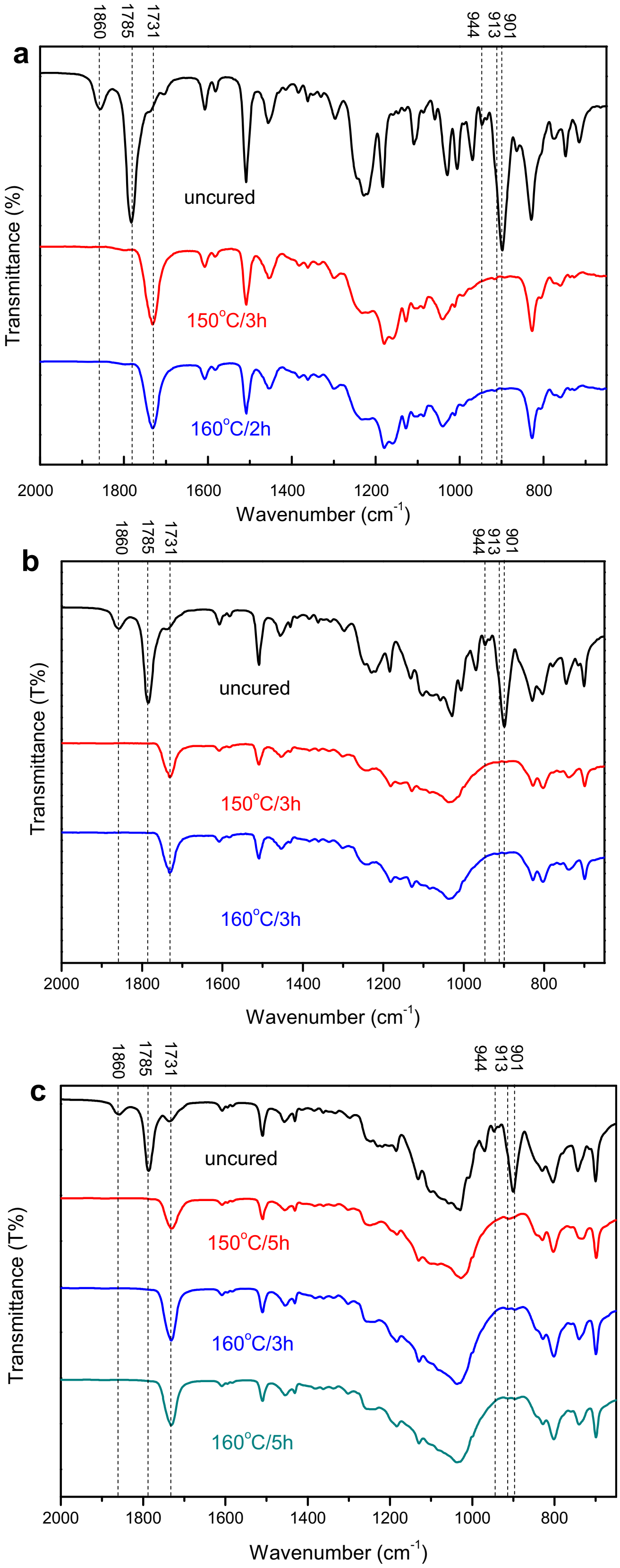

Fig. 2. FTIR spectra of (a) DGEBA–MHHPA, (b) DGEBA–PMSE-0.2, and (c) DGEBA–PMSE-0.4 under different postcuring conditions.

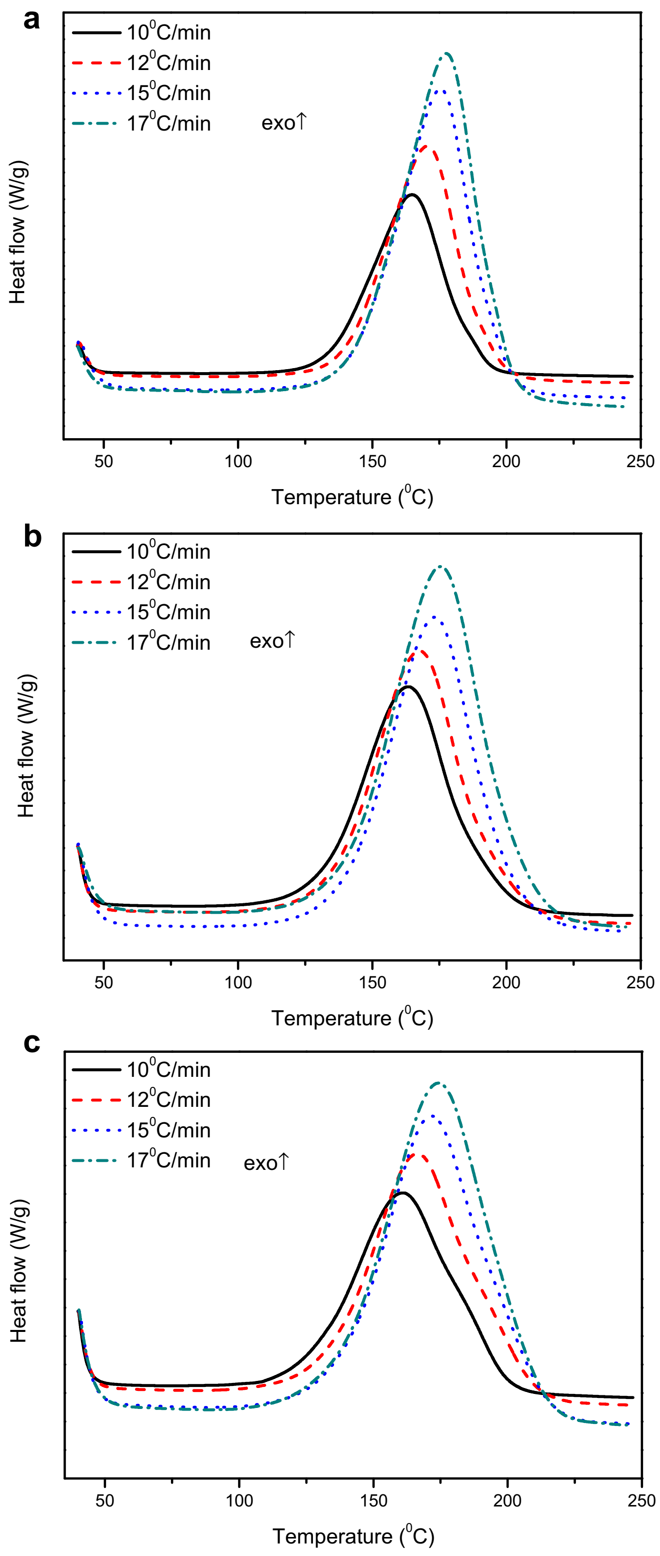

Fig. 3. DSC curves of (a) DGEBA–MHHPA, (b) DGEBA–PMSE-0.2, and (c) DGEBA–PMSE-0.4 at heating rates of 10, 12, 15, and 17 °C/min.

reaction was determined. The Kissinger method may be expressed as Eq. (1), where β is the linear heating rate, A is the pre-exponential factor, E is the activation energy, and R is the universal gas constant. The value of E may be obtained by means of a plot of $\ln(\beta/T_p^2)$ versus $1/T_p$.

Table 1
The peak temperature (T_p) for DSC at different heating rates and the activation energy (E) of reaction of the three materials.

	Heating rate β (°C/min)	T_p (°C)	E (KJ/mol)
DGEBA–MHHPA	10	164.9	60.9
	12	170.7	
	15	175.5	
	17	177.5	
DGEBA–PMSE-0.2	10	163.9	64.9
	12	167.9	
	15	173.4	
	17	175.6	
DGEBA–PMSE-0.4	10	163.3	69.4
	12	167.1	
	15	172.1	
	17	174.4	

$$\ln\left(\frac{\beta}{T_p^2}\right) = \ln\left(\frac{AR}{E}\right) - \frac{E}{RT_p} \tag{1}$$

Fig. 3 shows the exothermic curves of the three materials for four different heating rates of 10, 12, 15, and 17 °C min^{-1}. In Table 1, we summarize the heating rate, the peak temperature, and the activation energy of each reaction. The values of the activation energy of curing were 60.9, 64.9, and 69.4 kJ mol^{-1} for DGEBA–MHHPA, DGEBA–PMSE-0.2, and DGEBA–PMSE-0.4, respectively. Therefore, the order of reactivity of the curing reaction for the three materials is: DGEBA–MHHPA > DGEBA–PMSE-0.2 > DGEBA–PMSE-0.4. The implication is that the higher the amount of multifunctional PMSE, the lower the reactivity of the hybrids.

3.4. *Long-term thermal aging behavior*

3.4.1. *Optical properties*

The optical transparency of the plate samples was measured between 400 and 750 nm using a spectrophotometer, as shown in Fig. 4. All the hybrids were highly transparent, with transmittances higher than 88% in the range of visible wavelengths, namely 450–700 nm.

Fig. 5 shows the change in transmittance of the three materials over time. During the first 20 days of high temperature treatment,

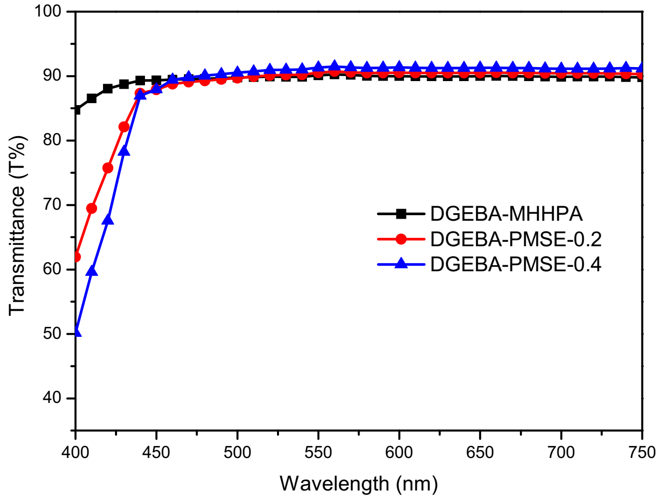

Fig. 4. Transmittance spectra of the plate samples of DGEBA–MHHPA, DGEBA–PMSE-0.2, and DGEBA–PMSE-0.4 before thermal aging.

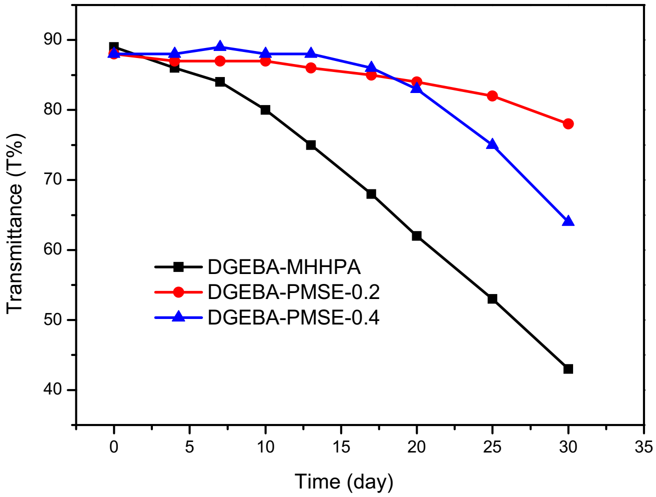

Fig. 5. The stability of transmittance at 450 nm of the plate samples of DGEBA–MHHPA, DGEBA–PMSE-0.2, and DGEBA–PMSE-0.4 against time for thermal aging at 150 °C.

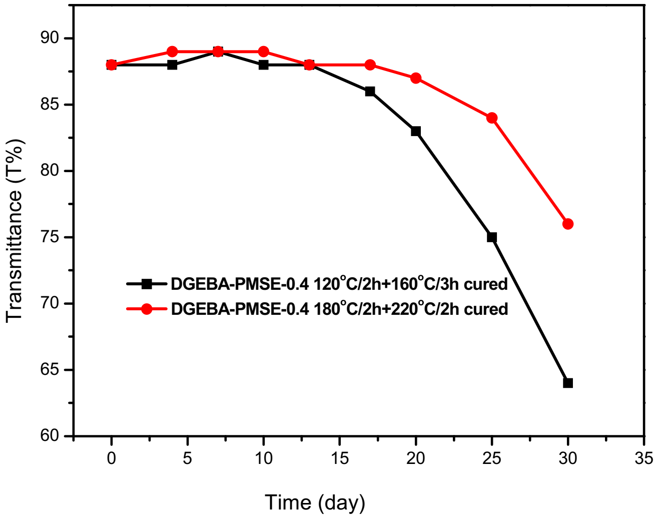

Fig. 6. The stability of transmittance at 450 nm of the plate samples of DGEBA–PMSE-0.4 for two curing profiles after thermal aging at 150 °C.

the reduction in transmittance of both DGEBA–PMES-0.2 and DGEBA–PMES-0.4 was less than 5%, whereas for DGEBA–MHHPA the reduction was 27% over the same period. After 30 days, the transmittances of DGEBA–PMES-0.2 and DGEBA–PMES-0.4 had reduced by 10 and 24%, respectively, and that of DGEBA–MHHPA had reduced by 46%. These results show that the thermal stability of the hybrids that contained PMSE was enhanced by the siloxane structure of the main chain.

The results in Fig. 5 show that the DGEBA–PMSE-0.4 hybrid was not the most thermally stable. Over the first 20 days, the transmittance of DGEBA–PMES-0.4 was reduced more than that of DGEBA–PMES-0.2. The DSC kinetic analysis showed that the presence of PMSE could hinder the curing reaction. It would be difficult to identify a small quantity of uncured functional group using FTIR, but this could have dissociated easily to form free radicals at high temperatures. As a result of the degradation mechanism of the polymer, DGEBA-type epoxies form many different types of chromophoric structure, including the yellow quinone structure [20,21]. The presence of free radicals enhances the formation of these types of chromophoric group. Furthermore, a very small amount of chromophoric group can cause a dramatic yellowing of the polymer. The greatest reduction in transmittance during thermal aging occurred in the range 400–450 nm. DGEBA–PMSE-0.4 might dissociate to form more free radicals than DGEBA–PMSE-0.2 because it has more uncured functional groups.

In view of the foregoing results, DGEBA–PMSE-0.4 was cured at a higher temperature (180 °C for 2h followed by 220 °C for 2h). The transmittance of DGEBA–PMSE-0.4 cured at a higher temperature had only decayed by 12% after 30 days thermal aging, and was compared with that of the DGEBA–PMSE-0.4 cured at a lower temperature, as shown in Fig. 6. The transmittance of DGEBA–PMSE-0.4 was more stable when it was cured at a higher temperature than at a lower curing temperature. However, such high temperatures can cause serious damage to the mold and the device, and therefore are not suitable for the manufacturing process.

3.4.2. Dynamic mechanical properties

The partial replacement of epoxy with PMSE is an effective means of improving the optical thermal stability of the material. DMA was used to measure the dynamic mechanical properties of the plate samples before and after long-term thermal aging had occurred.

The loss modulus (in MPa) was measured as a function of temperature and the results are shown in Fig. 7. Two relaxation peaks were apparent in the temperature range −100 to 280 °C. The peak at the higher temperature is the alpha transition temperature T_α, and the peak at the lower temperature is the beta transition temperature T_β. In this study, the values of T_β were all within the range −25 to −45 °C. The relaxation peaks signify the mobility of the polymer chains. In general, T_α is associated with the major transition of polymers and represents the change of the main segment from a glassy to a rubbery state. T_α is also known as T_g. T_β is associated with the motions of the local or side group segments of the polymer. The area under the relaxation peak represents the relaxation strength, which determines the activation barrier for deformation, flow or creep, change due to physical aging, and the diffusion of gas into the polymer, as reflected in the activation energies for the transition [22]. In other words, the relaxation peak is related to the strength of the response of the polymer to processes of this kind. Changes in the relaxation peak (and relaxation strength) imply a phase change in the polymer [23–25].

By inspection of Fig. 7(a), it may be seen that the value of T_α for DGEBA–MHHPA was 155 °C before thermal aging took place. After 30 days of thermal aging, T_α had increased to 162 °C. For DGEBA–PMSE-0.2, the value of T_α was 95 °C before thermal aging [Fig. 7(b)], and after 30 days, T_α had increased to 118 °C. Fig. 7(c) shows that for DGEBA–PMSE-0.4, the value of T_α was 55 °C before thermal aging. After thermal aging for 30 days, T_α had increased dramatically to 117 °C. In summary, after 30 days the value of T_α for DGEBA–PMSE-0.2 had increased by 23 °C, and for DGEBA–PMSE-0.4 it had increased by 62 °C, but for DGEBA–MHHPA the equivalent increase was less than 10 °C.

The changes in relaxation strength are summarized in Fig. 8. Fig. 8(a) shows that the relaxation strength associated with T_α increased by 111% after 30 days in the case of DGEBA–PMES-0.4, and by 30% in the case of DGEBA–PMES-0.2. However, the same amount of thermal aging caused the relaxation strength of T_α for DGEBA–MHHPA to change by less than 10%. Fig. 8(b) shows that thermal aging caused the relaxation strength associated with T_β to increase by 303% after 30 days in the case of DGEBA–PMES-0.4, but by less than 20% in the cases of DGEBA–PMES-0.2 and DGEBA–MHHHPA.

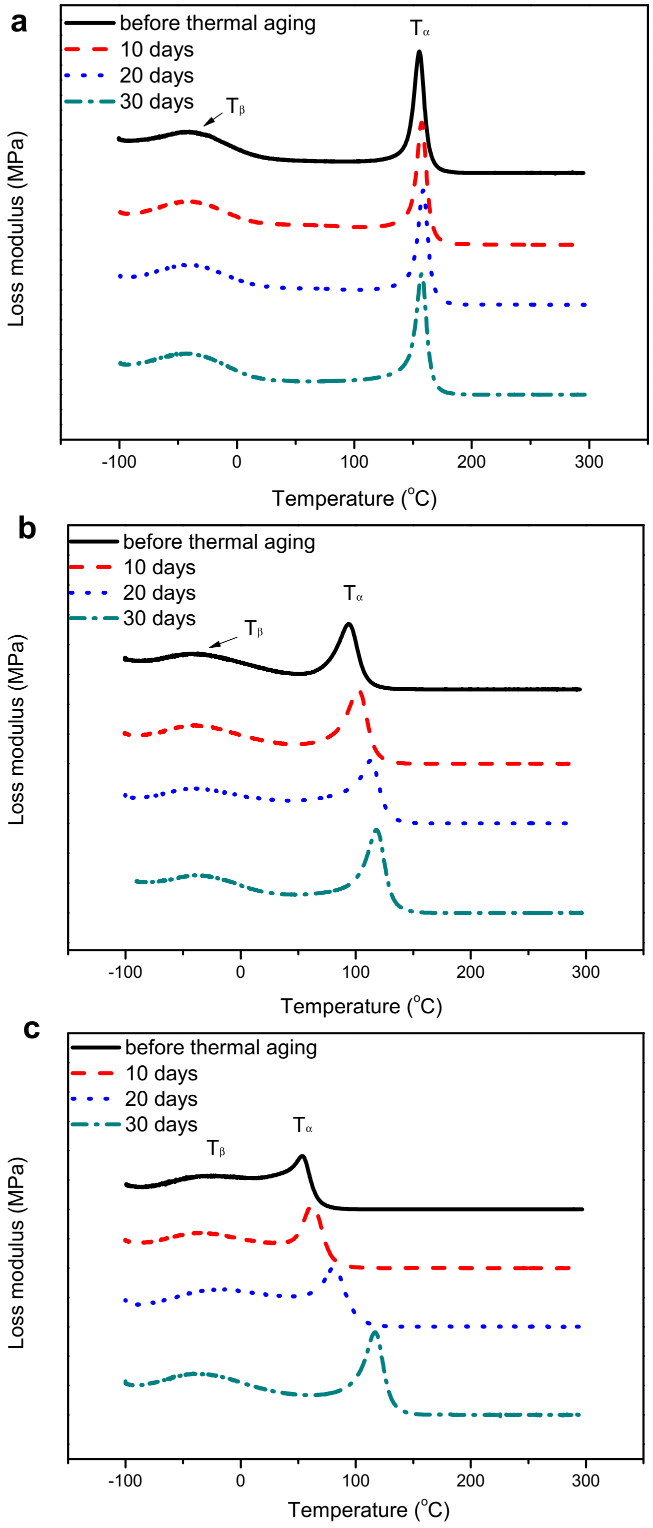

Fig. 7. The DMA curves of the loss moduli of (a) DGEBA–MHHPA, (b) DGEBA–PMSE-0.2, and (c) DGEBA–PMSE-0.4 after 0, 10, 20, and 30 days of thermal aging at 150 °C.

For DGEBA–MHHPA, the results show that 30 days of thermal aging caused the transmittance to decrease by 46%. However, the dynamic mechanical properties were unchanged, which revealed that the optical yellowing caused by the dissociation of the chemical bonds occurred earlier than the deterioration in the dynamic mechanical properties of the material.

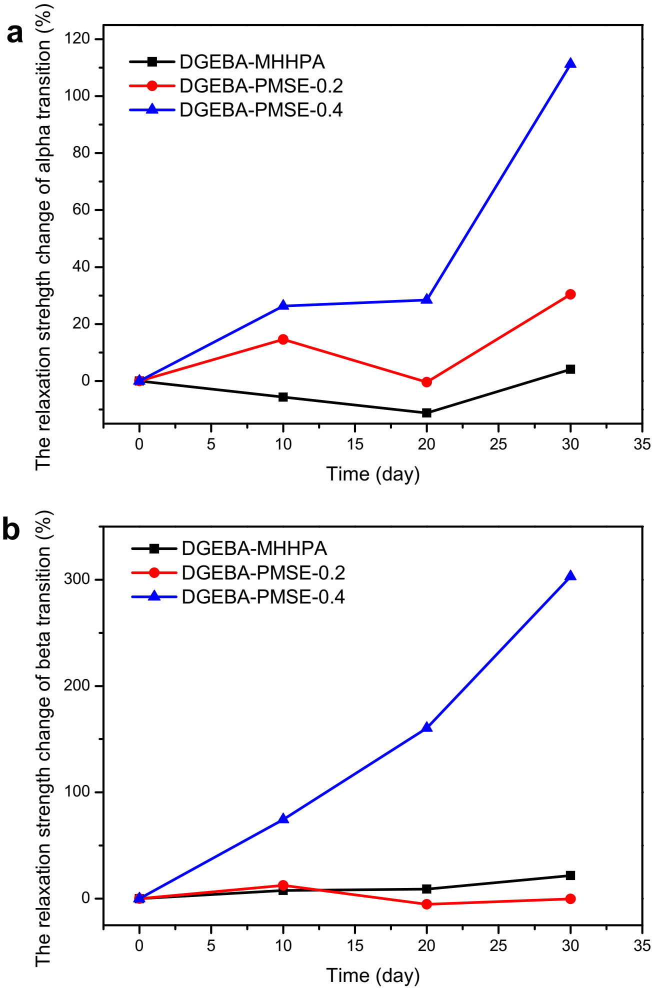

Fig. 8. The change in relaxation strength of the (a) alpha transition and (b) beta transition of the plate samples of DGEBA–MHHPA, DGEBA–PMSE-0.2, and DGEBA–PMSE-0.4 after 0, 10, 20, and 30 days of thermal aging at 150 °C.

The DGEBA–PMSE hybrids (especially DGEBA–PMSE-0.4) clearly underwent a molecular rearrangement during thermal aging, which increased with increasing PMSE content. After thermal aging, the hybrids were stiffer than the material in its original state.

3.4.3. *Morphology*

The morphological changes in the polymer on the nanoscale were observed using TEM [26–30]. TEM images of DGEBA–PMSE-0.2 and DGEBA–PMSE-0.4 before thermal aging are shown in Fig. 9 (a) and (b), respectively. The bright spots correspond to clusters formed by the aggregation of long carbon or siloxane chains, and the darker regions correspond to the aromatic domains. Fig. 9(a) shows a number of bright spots of approximately 3–20 nm in size, which are distributed homogeneously throughout DGEBA–PMSE-0.2. The bright spots in DGEBA–PMSE-0.4, shown in Fig. 9(b), were larger than those in DGEBA–PMSE-0.2, being approximately 20–50 nm. Thus, the sizes of the clusters depended on the amount of PMSE in the hybrids.

The changes in the molecular rearrangement of the DGEBA–PMSE hybrids that occurred during thermal aging may be seen in the TEM images of Fig. 10. Images of DEGBA-PMSE-0.2 after 0, 20, and 30 days of thermal aging are shown in Fig. 10 (a)–(c), and the equivalent images of DEGBA-PMSE-0.4 are shown in

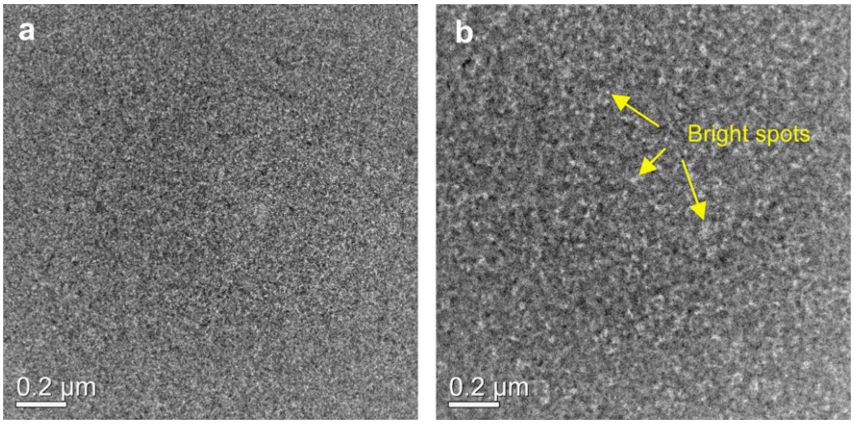

Fig. 9. The transmission electron micrographs of (a) DGEBA–PMSE-0.2 and (b) DGEBA–PMSE-0.4 before thermal aging.

Fig. 10(d)–(f). The bright spots reduced in size during thermal aging and disappeared altogether after 30 days. In each case, the hybrids became more miscible, and also more compact, than in their initial states as a result of the molecular rearrangement. The molecular rearrangement of the DGEBA–PMSE hybrids induced an increase in T_α, as well as an increase in relaxation strength.

3.4.4. The stability of LED light output

Thermal aging causes a reduction in the luminous flux of the LED, as shown in Fig. 11, where the luminous flux (normalized to its initial value) is plotted as a function of time. Two causes of this reduction may be inferred: (1) degradation of the LED device itself, and (2) thermal degradation of the encapsulant. In the first mechanism, heating of the junction causes a thermal stress to be induced in the LED device itself [31,32]. In the present study, a temperature of 150 °C was used to accelerate thermal aging and to mimic the working temperature of an LED. After 30 days, the luminous flux of the LEDs encapsulated by DGEBA–PMSE-0.2 and DGEBA–MHHPA had decreased by 59% and 78%, respectively. Use of DGEBA–PMSE hybrid as an encapsulant resulted in a 19% improvement in the light output as compared with DGEBA–MHHPA. The results showed that DGEBA–PMSE-0.2 performed better than DGEBA–MHHPA and DGEBA–PMSE-0.4 in terms of the stability of its luminous flux. After 30 days, the luminous flux of LEDs encapsulated by DGEBA–PMES-0.4 decreased by 81%, a figure that was similar to that for DGEBA–MHHPA. Although the optical properties of DGEBA–PMES-0.4 are more stable than those of DGEBA–MHHPA, LEDs encapsulated by this hybrid are not very stable.

The molecular rearrangement of the encapsulant is another factor that affects the performance of the LED. The DMA and TEM results showed that DGEBA–PMES-0.4 was subject to a greater degree of molecular rearrangement during thermal aging than DGEBA–PMSE-0.2, and the resulting increase in relaxation strength

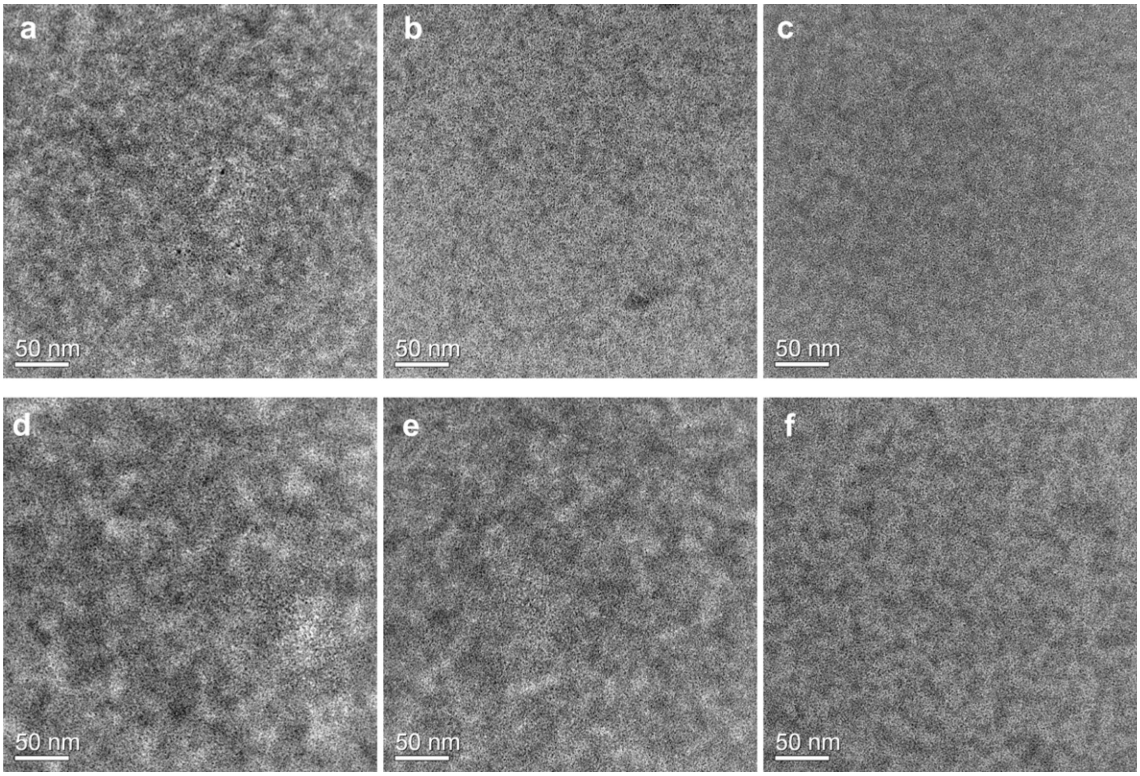

Fig. 10. The transmission electron micrographs of (a)–(c) DGEBA–PMSE-0.2 and (d)–(f) DGEBA–PMSE-0.4 after 0, 20, and 30 days of thermal aging at 150 °C.

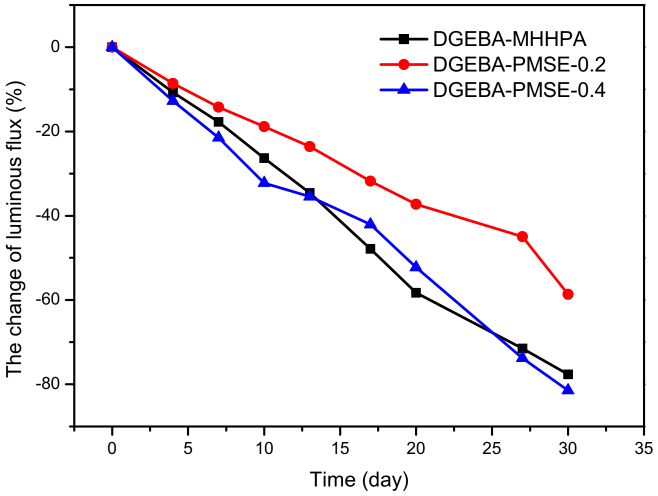

Fig. 11. The change of luminous flux of the LEDs encapsulated with DGEBA–MHHPA, DGEBA–PMSE-0.2, and DGEBA–PMSE-0.4 against time for thermal aging at 150 °C.

caused the hybrids to become stiffer. The stiffening of the material may induce thermal stress in the encapsulated LEDs, thereby affecting their stability.

In summary, in an organic–inorganic hybrid material that is used in an LED device, optical stability is not the only requirement for the stability of the luminous flux of LEDs. It is also necessary to consider the molecular rearrangement of the hybrids during thermal aging.

4. Conclusions

We have described herein our investigation of the effects of thermal aging on the optical and dynamic mechanical properties of transparent phenylmethylsiloxane-modified epoxy hybrids, together with the effect of any changes in these properties on the performance of encapsulated LEDs.

After long-term thermal aging at 150 °C, the DGEBA–PMSE hybrids were more thermally stable in their optical properties than DGEBA–MHHPA. DGEBA–MHHPA was subject to severe yellowing, while its dynamic mechanical properties remained stable. The material deteriorated optically much earlier than the dynamic mechanical properties degraded, and this affected the stability of the luminous flux of encapsulated LEDs.

The dynamic mechanical properties of the DEGBA-PMSE hybrids were altered as a result of thermal aging. DGEBA–PMES-0.4 was relatively thermally stable in optical terms, but the rearrangement of its molecules led to a stiffening of the material during thermal aging and caused the luminous flux of the encapsulated LEDs to degrade. The relative optical and dynamic mechanical stability of DGEBA–PMSE-0.2 afforded this material the most stable light output of all the encapsulated LEDs tested.

References

[1] Y. Morita, J. Appl. Polym. Sci. 97 (2005) 1395–1400.
[2] N. Narendran, Y. Gu, J.P. Freyssinier, H. Yu, L. Deng, J. Cryst. Growth 268 (2004) 449–456.
[3] C.F. Canto, A. De, L.A.S. Prado, E. Radovanovic, I.V.P. Yoshida, Polym. Eng. Sci. 48 (2008) 141–148.
[4] S.T. Lin, S.K. Huang, J. Polym. Sci., Part A: Polym. Chem. 34 (1996) 1907–1922.
[5] S. Ma, W. Liu, Z. Wang, C. Hu, C. Tang, Polym.-Plastics Technol. Eng. 49 (2010) 467–473.
[6] J. Tong, R. Bai, Y. Zou, C. Pan, S. Ichimura, J. Appl. Polym. Sci. 52 (1994) 1373–1381.
[7] S. Ma, W. Liu, Z. Wei, H. Li, J. Macromol. Sci., Part A: Pure and Appl. Chem. 47 (2010) 1084–1090.
[8] M. Gonzalez, P. Kadlec, P. Tepanek, A. Strachota, L. Matejka, Polymer 45 (2004) 5533–5541.
[9] S.S. Lee, S.C. Kim, J. Appl. Polym. Sci. 69 (1998) 1291–1300.
[10] S.S. Hou, Y.P. Chung, C.K. Chan, P.L. Kuo, Polymer 41 (2000) 3263–3272.
[11] J.C. Cabanelas, B. Serrano, M.G. Gonzalez, J. Baselga, Polymer 46 (2005) 6633–6639.
[12] J.S. Kim, S. Yang, B.S. Bae, Chem. Mater. 22 (2010) 3549–3555.
[13] Y. Morita, S. Tajima, H. Suzuki, H. Sugino, J. Appl. Polym. Sci. 109 (2008) 1808–1813.
[14] S.C. Yang, J.S. Kim, J.H. Jin, S.Y. Kwak, B.S. Bae, J. Appl. Polym. Sci. 117 (2010) 2140–2145.
[15] K.C. Chen, C.W. Hsu, H.T. Li, Mater. Res. Soc. Symp. Proc. 1007 (2007) 23–27.
[16] W. Huang, Y. Zhang, N. Yu, Y. Yuan, J. Appl. Polym. Sci. 104 (2007) 3954–3959.
[17] Y.Q. Li, Y. Yang, S.Y. Fu, Comp. Sci. Technol. 67 (2007) 3465–3471.
[18] H.E. Kissinger, Analyt. Chem. 29 (11) (1957) 1702–1706.
[19] Y. Liu, Z. Du, C. Zhang, C. Li, H. Li, J. Appl. Polym. Sci. (2007) 2041–2048.
[20] N. Grassie, M.I. Guy, N.H. Tennent, Polym. Degrad. Stab. 13 (1985) 11–20.
[21] N. Grassie, M.I. Guy, N.H. Tennent, Polym. Degrad. Stab. 12 (1985) 65–91.
[22] K.P. Menard, Dynamic Mechanical Analysis: A Practical Introduction, CRC, 1999.
[23] C. Sender, E. Dantras, L. Dantras-Laffont, M.H. Lacoste, J. Dandurand, M. Mauzac, J.L. Lacout, C. Lavergne, P. Demont, A. Bernes, C. Lacabanne, J. Biome. Mater. Res. – Part B Appl. Biomater. 83 (2007) 628–635.
[24] H. Liu, S. Zheng, K. Nie, Macromolecules 38 (2005) 5088–5097.
[25] A. Bobovitch, E. Gutman, S. Henning, G.H. Michler, J. Appl. Polym. Sci. 90 (2003) 3424–3429.
[26] C. Hedesiu, D.E. Demco, R. Kleppinger, G. Vanden Poel, W. Gijsbers, B. Blumich, K. Remerie, V.M. Litvinov, Macromolecules 40 (2007) 3977–3989.
[27] S. Rastogi, A.B. Spoelstra, J.G.P. Goossens, P.J. Lemstra, Macromolecules 30 (1997) 7880–7889.
[28] A. Kato, M. Nishioka, Y. Takahashi, T. Suda, H. Sawabe, A. Isoda, O. Drozdova, T. Hasegawa, T. Izumi, K. Nagata, S. Hikasa, H. Iwabuki, A. Asano, J. Appl. Polym. Sci. 116 (2010) 3056–3069.
[29] T.J. Savenije, J.E. Kroeze, X. Yang, J. Loos, Adv. Funct. Mater. 15 (2005) 1260–1266.
[30] A. Strachota, P. Whelan, J. Kriz, J. Brus, M. Urbanova, M. Iouf, L. Matejka, Polymer 48 (2007) 3041–3058.
[31] G. Zaeschmar, R.S. Speer, J. Appl. Phys. 50 (1979) 5686–5690.
[32] S.C. Yang, P. Lin, C.P. Wang, S.B. Huang, C.L. Chen, P.F. Chiang, A.T. Lee, M.T. Chu, Microelectrion. Reliab. 50 (2010) 959–964.